ACS APPLIED MATERIALS & INTERFACES

Research Article

Cite This: ACS Appl. Mater. Interfaces 2019, 11, 3181−3188

www.acsami.org

Design Strategy for the Controlled Generation of Cationic Frameworks and Ensuing Anion-Exchange Capabilities

Gabriel Brunet,[†] Koen Robeyns,[‡] Racheal P. S. Huynh,[§] Jian-Bin Lin,[§] Sean P. Collins,[†] Glenn A. Facey,[†] George K. H. Shimizu,[§] Tom K. Woo,[†] and Muralee Murugesu*[,†]

[†]Department of Chemistry and Biomolecular Sciences, University of Ottawa, Ottawa, Ontario K1N 6N5, Canada

[‡]Institute of Condensed Matter and Nanosciences (IMCN), Université catholique de Louvain, Place L. Pasteur 1, 1348 Louvain-la-Neuve, Belgium

[§]Department of Chemistry, University of Calgary, Calgary, Alberta T2N 1N4, Canada

Supporting Information

ABSTRACT: Cationic frameworks are an emerging class of exceptional solid adsorbents capable of encapsulating highly toxic and persistent anionic pollutants. The controlled generation of cationic frameworks, however, lags behind the abundant design strategies devised to control the structures and topologies of neutral frameworks. In this regard, we report a rational approach that allows the conversion of the synthetic approach toward constructing a neutral framework into one allowing for the synthesis of a cationic one without incurring any changes to the overall topology or the selected metal ion. We demonstrate that the replacement of a functional group on an organic linker that promotes a similar coordination mode, but bearing one less negative charge, can yield the systematic generation of cationic frameworks. Moreover, we confirm the cationic nature of the metal−organic frameworks through preliminary anion-exchange experiments and propose a method to retain permanent porosity in cationic frameworks through the use of strongly binding anions. Altogether, these results show great promise for the construction of tunable nanoporous frameworks capable of carrying out anion-exchange processes.

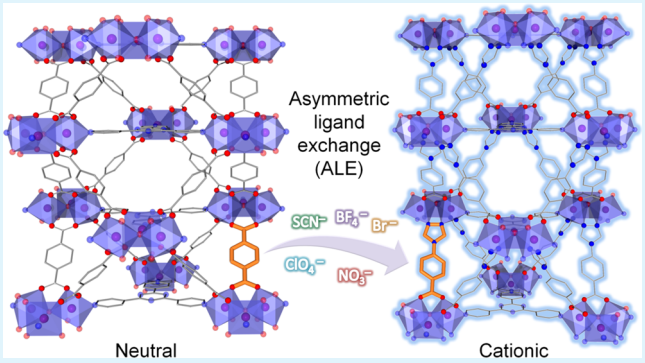

KEYWORDS: *cationic metal−organic frameworks, anion encapsulation, gas adsorption, binding energies, asymmetric ligand exchange*

INTRODUCTION

Research focused on metal−organic frameworks (MOFs) has been ongoing for a few decades; however, the intricacies related to this class of crystalline porous materials continue to be revealed to this day.[1−8] The development of MOFs is largely driven by the fact that they can encapsulate an impressive variety of guest molecules, ranging from greenhouse gases[9−11] to antitumoral and antiviral drugs.[12−14] Thus, multiple synthetic and design strategies have been devised over the years to promote specific structural topologies that can ultimately offer highly selective inclusion behaviors and predictable chemical transformations.[15−22] Among the many desired properties of MOFs, the capture of charged species has grown into an intense area of research because of the harmful impact of a number of ionic pollutants on human health and the environment.[23−40] The use of MOFs for ion-exchange applications is encouraged because of the fact that they can be obtained in both cationic and anionic forms, in contrast to other materials that are generally only obtainable in one form or the other (i.e., zeolites and layered double hydroxides).[41−50]

Recently, cationic frameworks have joined the forefront of ion-exchange technologies because of their potential ability to remove toxic anions such as ClO_4^-, AsO_4^{3-}, and $Cr_2O_7^{2-}$,[51−57] all of which are strictly regulated by the US Environmental Protection Agency during the purification of drinking water.[58] The initial strategy for obtaining a positively charged framework consisted of employing neutral polytopic organic ligands such as polypyridine- or imidazole-based linkers;[59−61] however, these structures generally elicited poor stability and limited tunability. Subsequent attempts to control ionicity were elegantly demonstrated by Bu and co-workers[62] in secondary building units consisting of planar trimers, where control over the oxidation state of the metal ions (M^{II} versus M^{III}) as well as the preemptive coordination of neutral ligands to the open metal sites of the trimer can indeed yield cationic frameworks. Similarly, the direct stripping of terminally coordinated F^- anions from the metal clusters of MOFs has also been shown to generate a cationic scaffolding.[63] With our goal of providing alternative routes to framework cationization, we report here an accessible and practical strategy for the systematic

Received: September 25, 2018
Accepted: December 28, 2018
Published: December 28, 2018

DOI: 10.1021/acsami.8b15946
ACS Appl. Mater. Interfaces 2019, 11, 3181−3188

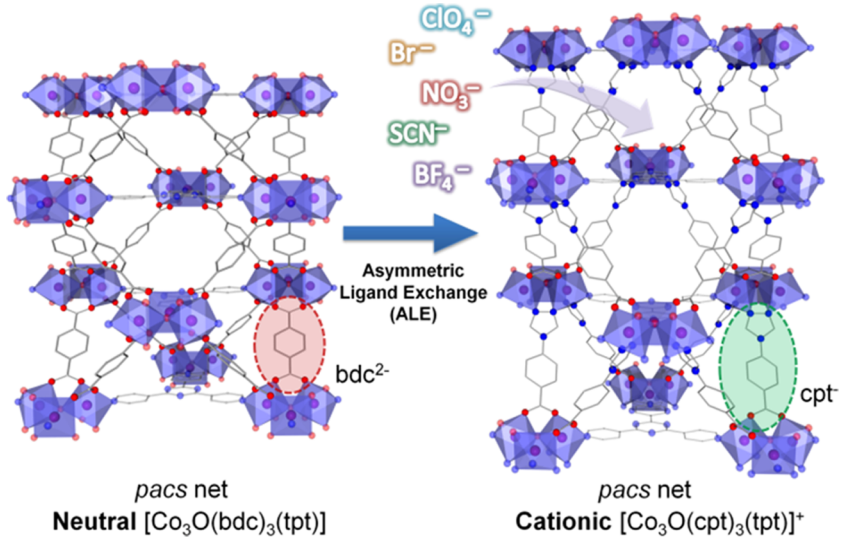

Figure 1. Depiction of the general ALE method for framework cationization, achieved by replacing a linear dicarboxylic acid linker with an asymmetric ligand containing a similar coordination mode but with one less negative charge (i.e., a triazole moiety).

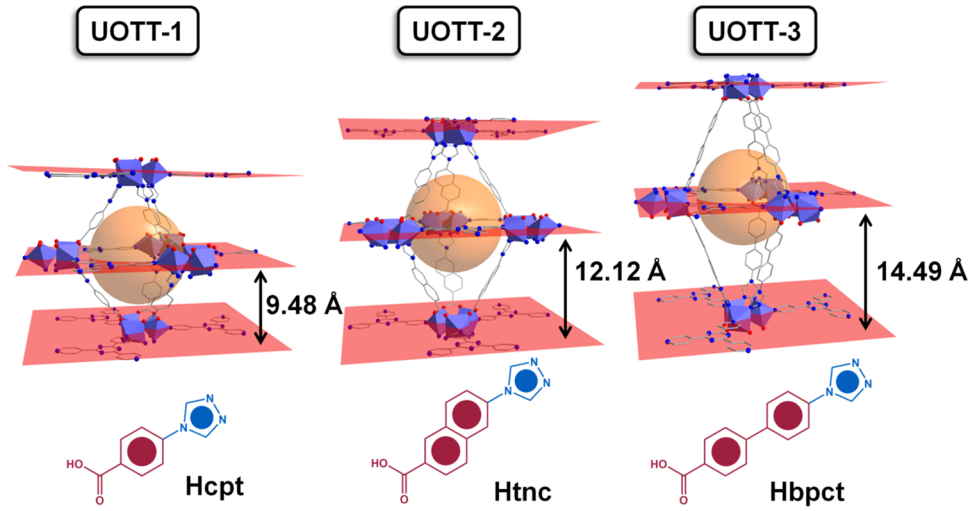

Figure 2. Structures of **UOTT-1**, **2**, and **3**, displaying the elongation of the charged framework with varying lengths of the asymmetric linker. Host–guest interactions can thus be tuned, along with their porosities and densities.

generation of cationic frameworks. This process involves replacing linear dicarboxylates, one of the most commonly used organic building blocks in MOF synthesis, with an asymmetric linker featuring a nearly identical coordination mode but with one less negative charge. More specifically, we have designed an asymmetric ligand-exchange (ALE) method, in which a carboxylic acid functionality is replaced by a 1,2,4-triazole moiety, effectively maintaining a similar binding mode that would permit an original and existing framework topology to be retained while also reducing the amount of negative charge on the organic building block (Figure 1). The strength of the present approach lies in its ability to control the charge of the framework while also retaining all of the benefits associated with the desired structural topology and reactivity of an existing neutral or anionic MOF. This can ultimately lead to the directed synthesis of high-performance ion-capturing materials.

Building on our previous work, where we employed the asymmetrically binding 4-(4′-carboxyphenyl)-1,2,4-triazole (Hcpt) ligand for constructing a variant of the iconic MIL-88 framework (*acs* type),[64] we have partitioned the pore spaces using the symmetry-matching tritopic 2,4,6-tri(4-pyridiyl)-1,3,5-triazine (tpt) ligand for implementing the ALE strategy. The linear dicarboxylates of the 9-connected trimers have been successfully replaced with three different asymmetric linkers of varying lengths (Figure 2), leading to an isoreticular series of MOFs with different pore sizes and densities (**UOTT-1**, **UOTT-2**, and **UOTT-3**, where UOTT stands for the University of Ottawa). We further demonstrate that control over the anions initially present in the pores can be achieved by employing different starting metal salts. Interestingly, direct visualization of the anions within the pore space, using single-crystal X-ray diffraction, reveals that these occupy symmetry-matching positions, thereby maintaining the necessary C_3 symmetry.[65] To the best of our knowledge, this is the first time guest molecules (solvents or counterions) have been located crystallographically in the *pacs*-MOF platform (*pacs* stands for partitioned *acs* net).[19,21,66] This offers invaluable insights into the host–guest interactions, a key criterion in the rational optimization of porous materials. In addition to this,

DOI: 10.1021/acsami.8b15946
ACS Appl. Mater. Interfaces 2019, 11, 3181−3188

Table 1. Single-Crystal X-ray Data for UOTT-1, 2, and 3

compound	formula[a]	*a*,*b* (Å)	*c* (Å)	space group	anion localized
NO_3@UOTT-1	$\{[Co_3(\mu_3\text{-}O)(cpt)_3(tpt)]\cdot NO_3\}_n$	16.7567(5)	19.0343(7)	$P6_3/mc$	yes
Br@UOTT-1	$\{[Co_3(\mu_3\text{-}O)(cpt)_3(tpt)]\cdot Br\}_n$	16.6968(9)	18.9684(10)	$P6_3/mc$	yes
NCS@UOTT-1	$\{[Co_3(\mu_3\text{-}O)(cpt)_3(tpt)]\cdot NCS\}_n$	16.8384(10)	19.0516(13)	$P6_3/mc$	yes
NO_3@UOTT-2	$\{[Co_3(\mu_3\text{-}O)(tnc)_3(tpt)]\cdot NO_3\}_n$	16.6264(7)	24.2500(13)	$P31c$	no
ClO_4@UOTT-2	$\{[Co_3(\mu_3\text{-}O)(tnc)_3(tpt)]\cdot ClO_4\}_n$	16.6138(8)	24.2258(12)	$P31c$	yes
NO_3@UOTT-3	$\{[Co_3(\mu_3\text{-}O)(bpct)_3(tpt)]\cdot NO_3\}_n$	16.6267(3)	28.9795(7)	$P6_3/mc$	yes
BF_4@UOTT-3	$\{[Co_3(\mu_3\text{-}O)(bpct)_3(tpt)]\cdot BF_4\}_n$	16.7599(5)	29.0651(9)	$P6_3/mc$	yes

[a]cpt = 4-(4′-carboxyphenyl)-1,2,4-triazole; tnc = 6-(4*H*-1,2,4-triazol-4-yl)-2-naphthoic acid; bpct = 4′-(4*H*-1,2,4-triazol-4-yl)biphenyl-4-carboxylic acid; and tpt = 2,4,6-tri(4-pyridyl)-1,3,5-triazine.

we have characterized the MOFs in terms of the affinity of small monoanions to the framework, the ease at which they can be replaced, and the effect of the binding strength of the anions on their permanent porosity. These materials, although unfortunately not stable in aqueous media, still display a near-complete exchange of BF_4^- for NCS^- anions, when run on a simple gravity filtration column of a packed bed of the MOF. As such, we successfully confirm the cationization process through proof-of-principle anion-exchange experiments. Although other highly stable and selective MOFs do exist for anion-exchange processes,[67−71] in this work, we focus on addressing the lack of synthetic strategies for obtaining topologically desired cationic frameworks.

EXPERIMENTAL SECTION

Synthesis. The Hcpt ligand was synthesized according to previously published procedures.[64] The Htnc and Hbpct ligands were obtained under similar microwave conditions as those for Hcpt. All described MOFs were synthesized under solvothermal conditions; full synthetic and experimental details can be found in the Supporting Information (SI).

Anion Exchange Procedure. In a typical experiment, the selected MOF (0.05 mmol) was immersed in 10 mL of $CHCl_3$, in which a tetrabutylammonium (TBA^+) salt (0.5 mmol) containing different anions such as NO_3^-, Br^-, NCS^-, ClO_4^-, and BF_4^- was dissolved. The MOF powders were characterized by Fourier transform infrared (FT-IR) spectroscopy at room temperature and without stirring, over a period of up to 24 h.

RESULTS AND DISCUSSION

Synthesis and Structural Characterization. Single-crystal X-ray diffraction studies reveal that all compounds investigated belong to either the trigonal or the hexagonal crystal system (Tables 1 and S1−S3). The first series of cationic MOFs (**UOTT-1**) presented in this work are assembled by combining the asymmetric 4-(4′-carboxyphenyl)-1,2,4-triazole (Hcpt) ligand and tritopic 2,4,6-tris(4-pyridyl)-1,3,5-triazine (tpt) ligands and differ in terms of their counteranions. To provide additional control on the cationic frameworks, we have synthesized and designed two new asymmetric ligands by expanding the Hcpt ligand central ring to naphthalene (Htnc; **UOTT-2**) and biphenyl moieties (Hbpct; **UOTT-3**). It is worth mentioning that, to the best of our knowledge, no structure has been reported with the two latter linkers (Htnc and Hbpct). This effectively yields an isoreticular family of charged frameworks, where anions of varying sizes and compositions can be contained within the porous network. Expansion of the MOF is clearly evidenced by the elongation of the *c*-axis length from ∼19 to 30 Å and the relatively constant *a*- and *b*-axis. In all cases, the Co_3 trimer is charge-balanced by a single monoanion residing in the pore space. Whereas this type of metal cluster topology is commonly attributed to a mixed di- and trivalent configuration for Fe, Co, and Ni,[72,73] the present compounds reveal that all three Co ions are in a +2 oxidation state. This is corroborated by bond valence sum calculations (i.e., Co1 = 1.90 for **NO_3@UOTT-1**) and charge considerations. Additionally, magnetic susceptibility measurements performed on **NCS@UOTT-1** are well within the expected range for three isolated high-spin Co^{II} ions (5.62 cm^3 K mol^{-1}) exhibiting significant magnetic anisotropy, with a room temperature χT value of 7.13 cm^3 K mol^{-1} (Figure S1). Two similar MOFs containing oxo-centered trinuclear $\{Co_3\}$ cores and coordinated to the Hcpt ligand also report all three cobalt ions being in a +2 oxidation state.[22,64]

With a carefully engineered series of cationic MOFs in hand, we turned our attention to their anion-exchange capabilities. Not only can the **UOTT-1−3** series be prepared with different anions based simply on the choice of starting cobalt salts, but also, the anions can be replaced postsynthetically through exchange experiments. The first indication of being able to encapsulate anions of varying sizes and nature was through direct crystallographic visualization. In fact, the Br^-, NSC^-, ClO_4^-, and BF_4^- anions were successfully refined owing in part to their large electron densities and highly ordered states. The NO_3^- anions were also localized in **NO_3@UOTT-1** and **NO_3@UOTT-3** because of their very high crystal quality, despite being disordered. The lower electron density of NO_3^-, in combination with somewhat poorer-diffracting crystals, made it more difficult to observe the anionic guest in **NO_3@UOTT-2**. The crystallographic studies reveal that the anions take up significantly different positions within the framework to both maintain the necessary symmetry and optimize the host−guest interactions. For example, the bromide anions in **Br@UOTT-1** are stabilized by multiple dipole−dipole interactions with H15 and H18, through distances of 2.95 and 2.74 Å, respectively, originating from the hydrogen atoms of either the benzene or the triazole ring of the Hcpt ligand (Figure S2). Comparatively, the NCS^- anions in **NCS@UOTT-1** sit above the trinuclear cluster and are linked to the triazole moieties through S···π interactions (Figure S3). Such host−guest interactions are strong and occur between the sulfur atom of NCS^- molecules and the centroid of adjacent triazole rings through a distance of 3.54 Å. In the case of **ClO_4@UOTT-2**, the ClO_4^- anions participate in anion···π interactions with the naphthalene rings of the tnc^- ligand (Figure S4). The perchlorates adopt three distinct crystallographic orientations in the lattice, with occupancy factors of 0.33. All three overlapping orientations experience anion−host interactions between an oxygen atom (O52, O53, or O55) and a centroid of a naphthalene ring. These weak interactions are

DOI: 10.1021/acsami.8b15946
ACS Appl. Mater. Interfaces 2019, 11, 3181−3188

characterized by an average oxygen···centroid distance of 3.59 Å. Additional host−anion interactions involving NO_3^- and BF_4^- anions are described in the SI (Figures S5−S7).

Kinetic Infrared Spectroscopy Study. Beyond the crystallographic evidence, the individual anions can also be confirmed by FT-IR spectroscopy, as shown in Figure 3.

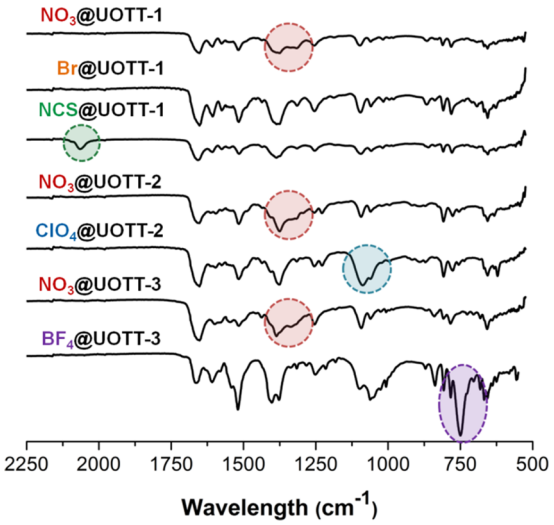

Figure 3. IR spectra of the as-synthesized MOFs, highlighting selected bands of the corresponding anions.

Characteristic bands belonging to NO_3^-, NSC^-, ClO_4^-, and BF_4^- anions are readily distinguished at ≈1390, 2068, 1090, and 754 cm^{-1}, respectively. To investigate anion affinity, we have selected the Hcpt-based frameworks and performed kinetic FT-IR studies, allowing us to directly probe the binding strength of the anions. In a typical experiment, samples of **UOTT-1** were immersed in a chloroform solution containing a different anion. By following the aforementioned bands through FT-IR spectroscopy, it is possible to observe the anion-exchange process, thus providing a means of determining the order of affinity of the guests (Figures S8−S16). To summarize these results, we have determined the following order of affinity of the guest anions: NCS^- > BF_4^- > Br^- > ClO_4^- > NO_3^-, as outlined in Table S4. Furthermore, these results are corroborated by the density functional theory (DFT)-calculated binding energies of the anions to the framework (*vide infra*). Interestingly, the incorporation of strongly binding NCS^- anions is accompanied by a drastic change in the color of the materials from orange to green. Thus, the presented compounds have the ability to act as visual colorimetric anion sensors for NCS^-. Due to the fact that a single monoanion is required to balance the charges, the optimal capacity of the **UOTT-1** materials ranges from 51.5 to 93.1 mg g^{-1} for the five anions studied.

Nuclear Magnetic Resonance Spectroscopy. To complement the FT-IR studies and to determine the exchange capacity of the MOF, we have performed a series of solid-state NMR (ssNMR) and solution NMR spectroscopy experiments. Accurate determination of the extent of ion exchange is critical in assessing the efficacy of a material for any industrial application. Here, we show that nearly 100% of the BF_4^- anions in **BF_4@UOTT-3** can be exchanged by NSC^-, and this can be achieved by simple gravity filtration of a tightly packed bed of the MOF (Figure S17). We have elected to perform these studies using BF_4^- anions because of the ease with which they can be monitored using NMR spectroscopy compared with other small monoanions (i.e., 100% natural abundance of ^{19}F). The ^{19}F magic-angle spinning (MAS) ssNMR spectrum of **BF_4@UOTT-3** was collected at room temperature before and after running the column. The initial material clearly reveals the presence of BF_4^- anions, with a peak centered at −161.6 ppm. Following anion exchange, by running a solution of tetrabutylammonium thiocyanate in chloroform through a packed bed of **BF_4@UOTT-3**, the resulting ^{19}F MAS ssNMR spectrum lacks all evidence of a peak for BF_4^- anions, suggesting that they have been fully exchanged. The anion-exchange process not only is essentially quantitative but also occurs on a short time scale. By exchanging only one of the two carboxylic acids within the organic linker for a triazole group, we ensure that a single monoanion is required to balance the charges. Therefore, we avoid filling the entirety of the pore space with anions, thus maintaining significant porosity, which in turn likely contributes to the fast exchange kinetics that is observed in both NMR and FT-IR. The broad band centered at approximately −136.0 ppm, present in both spectra, was confirmed as being probe background by running a blank under identical conditions, whereas NaF was used as an internal standard, should there have been a need for a quantitative estimate of the amount of remaining BF_4^- anions. To unequivocally confirm the anion-exchange process, ^{19}F NMR was also performed on the resulting solution that passed through the MOF column, clearly revealing the exchanged BF_4^- anions as two resonance peaks separated by 0.05 ppm. The low-frequency 1:1:1:1 quartet corresponds to $^{11}BF_4^-$, whereas the high-frequency resonance is an unresolved 1:1:1:1:1:1:1:1 septet, identified as $^{10}BF_4^-$. Moreover, the

Table 2. Summary of the N_2 Gas Sorption Data for the UOTT-1, UOTT-2, and UOTT-3 Families Using Optimal Activation Conditions[a]

compound code	calculated BET surface area (m^2 g^{-1})	experimental BET surface area (m^2 g^{-1})	anion-binding energy (kJ mol^{-1})	total pore volume (cm^3 g^{-1})
NO_3@UOTT-1	2202.5	474.1	61.8	0.305
Br@UOTT-1	2163.5	691.8	78.6	0.419
NCS@UOTT-1	2196.8	824.7	94.4	0.324
NO_3@UOTT-2	2638.6	24.9	34.8	0.029
ClO_4@UOTT-2	2541.7	836.0	66.9	0.339
NO_3@UOTT-3	3107.0	18.8	24.7	0.026
BF_4@UOTT-3	3034.7	508.2	41.5	0.259

[a]The experimental BET surface area values display a clear dependence on the strength of the anion-binding energies, as determined through DFT calculations.

DOI: 10.1021/acsami.8b15946
ACS Appl. Mater. Interfaces 2019, 11, 3181−3188

intensity ratio of 20:80 matches very well with the natural abundances of ^{10}B and ^{11}B, respectively.

Effect of the Anion-Binding Strength on N_2 Gas Adsorption Behaviors. As mentioned, cationic MOFs are generally less stable than their neutral counterparts. It is also tempting to gauge the robustness of a MOF based solely on the metal cation and organic linkers. Given the highly porous and tunable features of the present isoreticular MOFs, we sought to examine their ability to generate permanently porous structures and how different anions, with varying binding strengths, may impact this behavior. To gain further insight, we tested all MOFs under various activation conditions for N_2 gas sorption experiments. The optimal conditions consisted of exchanging the dimethylformamide solvent molecules with $CHCl_3$ and subsequent activation at 100 °C overnight. It should be noted that the activation of the as-synthesized samples at 150 °C, as reported for a closely related material,[74] resulted in the sublimation of a white product that was identified as the starting ligand. This is presumably due to the partial collapse of the cationic frameworks upon activation (*vide infra*). The Brunauer–Emmett–Teller (BET) surface areas obtained through the milder activation conditions and $CHCl_3$ solvent-exchange procedure are reported in Table 2. The lower-than-expected values further suggest partially collapsed structures upon activation. Nevertheless, the N_2 sorption isotherms indicate that all samples, with the exception of **NO_3@UOTT-2** and **NO_3@UOTT-3**, display permanent porosity (Figure 4) and a dependence of the porosity on the anion present. This is further substantiated by powder X-ray diffraction data (Figures S18–S24), where we observe a significant loss in the crystallinity and long-range order of the two aforementioned samples upon activation. Interestingly, the use of different anions in the frameworks of **UOTT-2** and **UOTT-3** (instead of NO_3^-) allows the retention of porosity as in the case of **ClO_4@UOTT-2** and **BF_4@UOTT-3**. In fact, these findings, in conjunction with other recently reported cationic frameworks,[75] suggest that more strongly binding anions limit the contraction of the framework upon activation and allow the frameworks to better retain porosity. Indeed, the binding energies of the anions and their respective frameworks were calculated by DFT (Table 2), which revealed that the NO_3^- anions continually give the lowest binding energies. Within the **UOTT-1** family, the significant difference in the experimental BET surface area among the three different anions (NO_3^-, Br^-, and NCS^-) cannot be explained simply by their varying sizes and geometries. It is noteworthy that there is a clear trend between the DFT-calculated binding energies and the experimental BET surface areas, where the more strongly binding anions result in markedly higher surface areas. Further evidence of the importance of the binding strength of the anions for maintaining porosity can be observed in the shape of the N_2 isotherms. The more weakly bound anions display hysteresis, whereas this behavior is absent in the more strongly bound anions. Such a feature presumably originates from the reorientation of the anions to better accommodate the gaseous molecules and is reinforced by the fact that the opening of the hysteresis is greatest in the weakest bound anion (NO_3^-). We cannot, however, entirely rule out the possibility of a phase change upon gas loading.

It was also found that the larger MOF variants led to lower binding energies, as expected. The binding energies for NO_3^- decrease from 61.8 to 34.8 and 24.7 kJ mol^{-1} when going from **UOTT-1** to **UOTT-2** and **UOTT-3**, respectively. This may explain why **NO_3@UOTT-1** retains porosity, whereas **NO_3@UOTT-2** and **NO_3@UOTT-3** exhibit significant structural collapse upon activation. In fact, within this family of MOFs, it appears that an anion would require a binding energy of >40 kJ mol^{-1} to keep the pores open upon activation. Furthermore, the calculated binding energies confirm the previously established trend of anion affinity (*vide supra*), with NCS^- being the most strongly bound anion (94.4 kJ mol^{-1}). Overall, this represents a rare example where permanent porosity can be tuned via the anion-exchange process and provides an avenue toward tuning the structural stability of cationic frameworks. As such, we demonstrate that the exchange of weakly bound anions, such as NO_3^- ions in this case, with more strongly binding anions provides a facile avenue to retain porosity. Therefore, we can foresee overcoming some of the

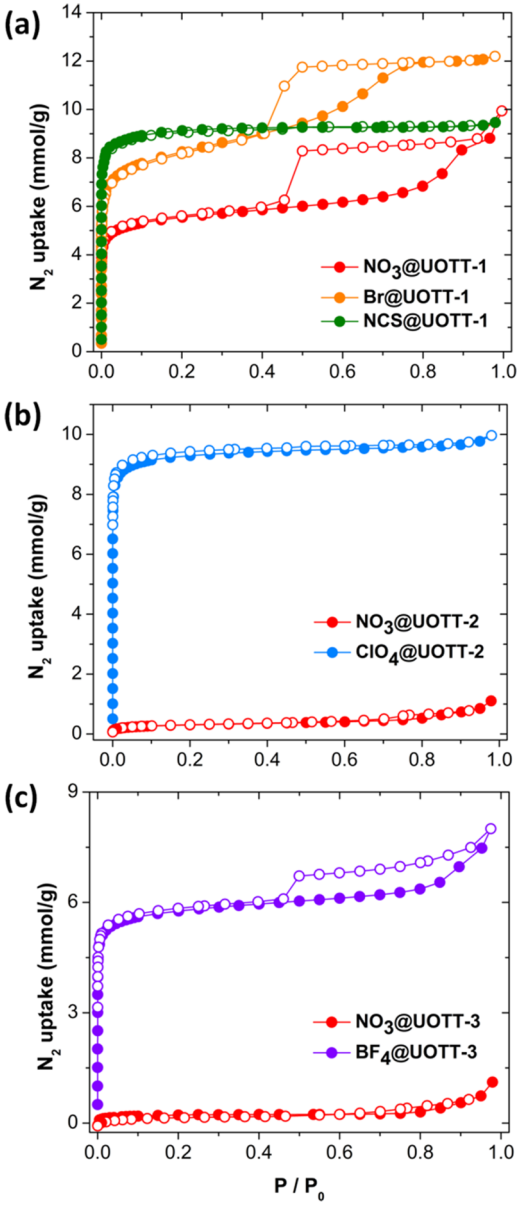

Figure 4. N_2 adsorption isotherms for the **UOTT-1** (a), **UOTT-2** (b), and **UOTT-3** (c) series, obtained at 77 K. The isotherms suggest a strong dependence of the porosity upon the binding strength of the anion. The presence of hysteresis in the more weakly bound anions may be attributed to the mobility and reorientation of the anions upon gas loading.

DOI: 10.1021/acsami.8b15946
ACS Appl. Mater. Interfaces 2019, 11, 3181–3188

porosity limitations that have frequently been plaguing cationic MOFs.

CONCLUSIONS

In this work, we have demonstrated a strategy that allows for the generation of a charged framework without any alterations to the desired topology or metal ions. Furthermore, we have shown the importance of the anion-binding strength in tuning the porosity of such materials, which is vital in retaining the desirable features of MOFs. An increase in the binding strength of the anion allows the cationic frameworks to display improved surface areas. In this family of MOFs, a binding strength of >40 kJ mol^{-1} appears to be required to maintain porosity. In addition to this, we can envision further tuning of the *pacs* platform using a combination of techniques, such as the pore-space partition and the ALE strategy, allowing for an optimization of the hydrophobicity and basicity of the organic linkers, which may lead to desired hydrolytic stability. Here, the ALE method joins a limited group of strategies for framework ionization that targets exciting applications encompassing anionic drug delivery and chemical sensing. This proof-of-principle study, where a series of cationic frameworks have been rationally constructed, can serve as a blueprint toward the design of high-performance anion-exchange materials.

ASSOCIATED CONTENT

Supporting Information

The Supporting Information is available free of charge on the ACS Publications website at DOI: 10.1021/acsami.8b15946.

Experimental and computational details, crystallographic data, magnetic plots, host–guest interactions, FT-IR studies, NMR spectroscopy, and powder X-ray diffraction patterns (PDF)

Structure factors for different data blocks (ZIP)

AUTHOR INFORMATION

Corresponding Author

*E-mail: m.murugesu@uottawa.ca.

ORCID

Gabriel Brunet: 0000-0001-9846-7845

George K. H. Shimizu: 0000-0003-3697-9890

Tom K. Woo: 0000-0003-0073-3901

Muralee Murugesu: 0000-0002-5123-374X

Notes

The authors declare no competing financial interest.

ACKNOWLEDGMENTS

We thank the Natural Sciences and Engineering Research Council of Canada (Discovery and DND Discovery Grant and Accelerator Supplements) for generous financial support and the University of Ottawa for essential infrastructure. G.B. gratefully acknowledges the support from NSERC (CGS-D).

REFERENCES

(1) Bennett, T. D.; Cheetham, A. K.; Fuchs, A. H.; Coudert, F.-X. Interplay Between Defects, Disorder and Flexibility in Metal-Organic Frameworks. *Nat. Chem.* **2016**, *9*, 11–16.

(2) Kim, H.; Yang, S.; Rao, S. R.; Narayanan, S.; Kapustin, E. A.; Furukawa, H.; Umans, A. S.; Yaghi, O. M.; Wang, E. N. Water Harvesting from Air with Metal-Organic Frameworks Powered by Natural Sunlight. *Science* **2017**, *356*, 430–434.

(3) Zhao, M.; Yuan, K.; Wang, Y.; Li, G.; Guo, J.; Gu, L.; Hu, W.; Zhao, H.; Tang, Z. Metal-Organic Frameworks as Selectivity Regulators for Hydrogenation Reactions. *Nature* **2016**, *539*, 76–80.

(4) Hendon, C. H.; Rieth, A. J.; Korzzyński, M. D.; Dincă, M. Grand Challenges and Future Opportunities for Metal-Organic Frameworks. *ACS Cent. Sci.* **2017**, *3*, 554–563.

(5) Marshall, R. J.; Kalinovskyy, Y.; Griffin, S. L.; Wilson, C.; Blight, B. A.; Forgan, R. S. Functional Versatility of a Series of Zr Metal-Organic Frameworks Probed by Solid-State Photoluminescence Spectroscopy. *J. Am. Chem. Soc.* **2017**, *139*, 6253–6260.

(6) Gallagher, A. T.; Lee, J. Y.; Kathiresan, V.; Anderson, J. S.; Hoffman, B. M.; Harris, D. T. A Structurally-Characterized Peroxomanganese(IV) Porphyrin from Reversible O_2 Binding within a Metal-Organic Framework. *Chem. Sci.* **2018**, *9*, 1596–1603.

(7) Julien, P. A.; Mottillo, C.; Friščić, T. Metal-Organic Frameworks Meet Scalable and Sustainable Synthesis. *Green Chem.* **2017**, *19*, 2729–2747.

(8) Zhang, W.; Lu, G.; Cui, C.; Liu, Y.; Li, S.; Yan, W.; Xing, C.; Chi, Y. R.; Yang, Y.; Huo, F. A Family of Metal-Organic Frameworks Exhibiting Size-Selective Catalysis with Encapsulated Noble-Metal Nanoparticles. *Adv. Mater.* **2014**, *26*, 4056–4060.

(9) Liu, J.; Thallapally, P. K.; Peter McGrail, B.; Brown, D. R.; Liu, J. Progress in Adsorption-Based CO_2 capture by Metal-Organic Frameworks. *Chem. Soc. Rev.* **2012**, *41*, 2308–2322.

(10) Shekhah, O.; Belmabkhout, Y.; Chen, Z.; Guillerm, V.; Cairns, A.; Adil, K.; Eddaoudi, M. Made-to-Order Metal-Organic Frameworks for Trace Carbon Dioxide Removal and Air Capture. *Nat. Commun.* **2014**, No. 4228.

(11) Vaidhyanathan, R.; Iremonger, S. S.; Shimizu, G. K. H.; Boyd, P. G.; Alavi, S.; Woo, T. K. Direct Observation and Quantification of CO_2 Binding Within an Amine-Functionalized Nanoporous Solid. *Science* **2010**, *330*, 650–653.

(12) Horcajada, P.; Gref, R.; Baati, T.; Allan, P. K.; Maurin, G.; Couvreur, P.; Férey, G.; Morris, R. E.; Serre, C. Metal-Organic Frameworks in Biomedicine. *Chem. Rev.* **2012**, *112*, 1232–1268.

(13) He, C.; Lu, K.; Liu, D.; Lin, W. Nanoscale Metal-Organic Frameworks for the Co-Delivery of Cisplatin and Pooled siRNAs to Enhance Therapeutic Efficacy in Drug-Resistant Ovarian Cancer Cells. *J. Am. Chem. Soc.* **2014**, *136*, 5181–5184.

(14) Hu, Q.; Yu, J.; Liu, M.; Dou, Z.; Yang, Y.; et al. A Low Cytotoxic Cationic Metal-Organic Framework Carrier for Controllable Drug Release. *J. Med. Chem.* **2014**, *57*, 5679–5685.

(15) Aulakh, D.; Varghese, J. R.; Wriedt, M. A New Design Strategy to Access Zwitterionic Metal-Organic Frameworks from Anionic Viologen Derivates. *Inorg. Chem.* **2015**, *54*, 1756–1764.

(16) Islamoglu, T.; Goswani, S.; Li, Z.; Howarth, A. J.; Farha, O. K.; Hupp, J. T. Postsynthetic Tuning of Metal-Organic Frameworks for Targeted Applications. *Acc. Chem. Res.* **2017**, *50*, 805–813.

(17) Zhou, H.-C.; Kitagawa, S. Metal-Organic Frameworks (MOFs). *Chem. Soc. Rev.* **2014**, *43*, 5415–5418.

(18) Sumida, K.; Stück, D.; Mino, L.; Chai, J.-D.; Bloch, E. D.; Zavorotynska, O.; Murray, L. J.; Dincă, M.; Chavan, S.; Bordiga, S.; Head-Gordon, M.; Long, J. R. Impact of Metal and Anion Substitution on the Hydrogen Storage Properties of M-BTT Metal-Organic Frameworks. *J. Am. Chem. Soc.* **2013**, *135*, 1083–1091.

(19) Zhao, X.; Bu, X.; Zhai, Q.-G.; Tran, H.; Feng, P. Pore Space Partition by Symmetry-Matching Regulated Ligand Insertion and Dramatic Tuning on Carbon Dioxide Uptake. *J. Am. Chem. Soc.* **2015**, *137*, 1396–1399.

(20) Kannappan, R.; Bucher, C.; Saint-Aman, E.; Moutet, J.-C.; Milet, A.; Oltean, M.; Métay, E.; Pellet-Rostaing, S.; Lemaire, M.; Chaix, C. Viologen-based Redox-Switchable Anion-Binding Receptors. *New. J. Chem.* **2010**, *34*, 1373–1386.

(21) Zhai, Q.-G.; Bu, X.; Zhao, X.; Li, D.-S.; Feng, P. Pore Space Partition in Metal-Organic Frameworks. *Acc. Chem. Res.* **2017**, *50*, 407–417.

(22) Chen, D.-M.; Tian, J.-Y.; Liu, C.-S.; Du, M. A Bracket Approach to Improve the Stability and Gas Sorption Performance of a

Metal-Organic Framework via in situ Incorporating the Size-Matching Molecular Building Blocks. *Chem. Commun.* **2016**, *52*, 8413−8416.
(23) Mandal, T. N.; Karmakar, A.; Sharma, S.; Ghosh, S. K. Metal-Organic Frameworks (MOFs) as Functional Supramolecular Architectures for Anion Recognition and Sensing. *Chem. Rec.* **2018**, *18*, 154−164.
(24) Ji, X.; Wu, R.-T.; Long, L.; Guo, C.; Khashab, N. M.; Huang, F.; Sessler, J. L. Physical Removal of Anions from Aqueous Media by Means of a Macrocycle-Containing Polymeric Network. *J. Am. Chem. Soc.* **2018**, *140*, 2777−2780.
(25) Manna, B.; Chaudhari, A. K.; Joarder, B.; Karmakar, A.; Ghosh, S. K. Dynamic Structural Behaviour and Anion-Responsive Tunable Luminescence of a Flexible Cationic Metal-Organic Framework. *Angew. Chem., Int. Ed.* **2013**, *52*, 998−1002.
(26) Li, X.; Xu, H.; Kong, F.; Wang, R. A Cationic Metal-Organic Framework Consisting of Nanoscale Cages: Capture, Separation, and Luminescence Probing of $Cr_2O_7^{2-}$ through a Single-Crystal to Single-Crystal Process. *Angew. Chem., Int. Ed.* **2013**, *52*, 13769−13773.
(27) Howarth, A. J.; Katz, M. J.; Wang, T. C.; Platero-Prats, A. E.; Chapman, K. W.; Hupp, J. T.; Farha, O. K. High Efficiency Adsorption and Removal of Selenate and Selenite from Water Using Metal-Organic Frameworks. *J. Am. Chem. Soc.* **2015**, *137*, 7488−7494.
(28) Li, Y.; Yang, Z.; Wang, Y.; Bai, Z.; Zheng, T.; Dai, X.; Liu, S.; Gui, D.; Liu, W.; Chen, M.; Chen, L.; Diwu, L.; Zhu, L.; Zhou, R.; Chai, Z.; Albretch-Schmitt, T. E.; Wang, S. A Mesoporous Cationic Thorium-Organic Framework that Rapidly Traps Anionic Persistent Organic Pollutants. *Nat. Commun.* **2017**, *8*, No. 1354.
(29) Zhang, Q.; Yu, J.; Cai, J.; Zhang, L.; Cui, Y.; Yang, Y.; Chen, B.; Qian, G. A Porous Zr-Cluster-based Cationic Metal-Organic Framework for Highly Efficient $Cr_2O_7^{2-}$ Removal from Water. *Chem. Commun.* **2015**, *51*, 14732−14734.
(30) Song, B.-Q.; Wang, X.-L.; Zhang, Y.-T.; Wu, X.-S.; Liu, H.-S.; Shao, K.-Z.; Su, Z.-M. Periodic Tiling of Triangular and Square Nanotubes in a Cationic Metal-Organic Framework for Selective Anion Exchange. *Chem. Commun.* **2015**, *51*, 9515−9518.
(31) Fei, H.; Han, C. S.; Robins, J. C.; Oliver, S. R. J. A Cationic Metal-Organic Solid Solution Based on Co(II) and Zn(II) for Chromate Trapping. *Chem. Mater.* **2013**, *25*, 647−652.
(32) Li, Z.; Li, H.; Guan, X.; Tang, J.; Yusran, Y.; Li, Z.; Xue, M.; Fang, Q.; Yan, Y.; Valtchev, V.; Qiu, S. Three-Dimensional Ionic Covalent Organic Frameworks for Rapid, Reversible, and Selective Ion Exchange. *J. Am. Chem. Soc.* **2017**, *139*, 17771−17774.
(33) Li, J.; Wang, X.; Zhao, G.; Chen, C.; Chai, Z.; Alsaedi, A.; Hayat, T.; Wang, X. Metal-Organic Framework-based Materials: Superior Adsorbents for the Capture of Toxic and Radioactive Metal Ions. *Chem. Soc. Rev.* **2018**, *47*, 2322−2356.
(34) Drout, R. J.; Otake, K.; Howarth, A. J.; Islamoglu, T.; Zhu, L.; Xiao, C.; Wang, S.; Farha, O. K. Efficient Capture of Perrhenate and Pertechnetate by a Mesoporous Zr Metal-Organic Framework and Examination of Anion Binding Motifs. *Chem. Mater.* **2018**, *30*, 1277−1284.
(35) Patino, M. A.; Smith, T.; Zhang, W.; Halasyamani, P. S.; Hayward, M. A. Cation Exchange in a 3D Perovskite—Synthesis of $Ni_{0.5}TaO_3$. *Inorg. Chem.* **2014**, *53*, 8020−8024.
(36) Bai, Z.; Wang, Y.; Li, Y.; Liu, W.; Chen, L.; Sheng, D.; Diwu, J.; Chai, Z.; Albrecht-Schmitt, T. E.; Wang, S. First Cationic Uranyl-Organic Framework with Anion-Exchange Capabilities. *Inorg. Chem.* **2016**, *55*, 6358−6360.
(37) Beck, S.; Lieber, S.; Schaper, F.; Geyer, A.; Brintzinger, H.-H. Anion Exchange in Alkyl-Zirconocene Borate Ion Pairs. Are Solvated Alkyl-Zirconocene Cations Relevant Intermediates? *J. Am. Chem. Soc.* **2001**, *123*, 1483−1489.
(38) Ok, K. M.; Baek, J.; Halasyamani, P. S.; O'Hare, D. New Layered Uranium Phosphates Fluorides: Syntheses, Structures, Characterizations, and Ion-Exchange Properties of $A(UO_2)F(HPO_4)\cdot xH_2O$ ($A = Cs^+, Rb^+, K^+$; $x = 0-1$). *Inorg. Chem.* **2006**, *45*, 10207−10214.
(39) Li, J.; Dai, X.; Zhu, L.; Xu, C.; Zhang, D.; Silver, M. A.; Li, P.; Chen, L.; Li, Y.; Zuo, D.; Zhang, H.; Xiao, C.; Chen, J.; Diwu, J.; Farha, O. K.; Albrecht-Schmitt, T. E.; Chai, Z.; Wang, S. $^{99}TcO_4^-$ Remediation by a Cationic Polymeric Framework. *Nat. Commun.* **2018**, *9*, No. 3007.
(40) Zhu, L.; Sheng, D.; Xu, C.; Dai, X.; Silver, M. A.; Li, J.; Li, P.; Wang, Y.; Wang, Y.; Chen, L.; Xiao, C.; Chen, J.; Zhou, R.; Zhang, C.; Farha, O. K.; Chai, Z.; Albrecht-Schmitt, T. E.; Wang, S. Identifying the Recognition Site for Selective Trapping of $^{99}TcO_4^-$ in a Hydrolytically Stable and Radiation Resistant Cationic Metal-Organic Framework. *J. Am. Chem. Soc.* **2017**, *139*, 14873−14876.
(41) Liu, Z.; Ma, R.; Osada, M.; Iyi, N.; Ebina, Y.; Takada, K.; Sasaki, T. Synthesis, Anion Exchange, and Delamination of Co−Al Layered Double Hydroxide: Assembly of the Exfoliated Nanosheet/Polyanion Composite Films and Magneto-Optical Studies. *J. Am. Chem. Soc.* **2006**, *128*, 4872−4880.
(42) Goh, K.-H.; Lim, T.-T.; Dong, Z. Application of Layered Double Hydroxides for Removal of Oxyanions: A Review. *Water Res.* **2008**, *42*, 1343−1368.
(43) Meyn, M.; Beneke, K.; Lagaly, G. Anion-Exchange Reactions of Layered Double Hydroxides. *Inorg. Chem.* **1990**, *29*, 5201−5207.
(44) Sels, B.; De Vos, D.; Buntinx, M.; Pierard, F.; Mesmaeker, A. K.-D.; Jacobs, P. Layered Double Hydroxides Exchanged with Tungstate as Biomimetic Catalysts for Mild Oxidative Bromination. *Nature* **1999**, *400*, 855−857.
(45) Fogg, A. M.; Dunn, J. S.; Shyu, S.-G.; Cary, D. R.; O'Hare, D. Selective Ion-Exchange Intercalation of Isomeric Dicarboxylate Anions into the Layered Doubled Hydroxide $[LiAl_2(OH)_6]Cl\cdot H_2O$. *Chem. Mater.* **1998**, *10*, 351−355.
(46) Haggerty, G. M.; Bowman, R. S. Sorption of Chromate and Other Inorganic Anions by Organo-Zeolite. *Environ. Sci. Technol.* **1994**, *28*, 452−458.
(47) Yusof, A. M.; Malek, N. A. N. N. Removal of Cr(IV) and As(V) from Aqueous Solutions by HDTMA-Modified Zeolite Y. *J. Hazard. Mater.* **2009**, *162*, 1019−1024.
(48) Liu, X.; Ravon, U.; Tuel, A. Evidence for F-/SiO- Anion Exchange in the Framework of As-Synthesized All-Silica Zeolites. *Angew. Chem., Int. Ed.* **2011**, *50*, 5900−5903.
(49) Tran, D. T.; Zavalij, P. Y.; Oliver, S. R. J. $Pb_3F_5NO_3$, a Cationic Layered Material for Anion-Exchange. *J. Am. Chem. Soc.* **2002**, *124*, 3966−3969.
(50) Geng, F.; Ma, R.; Sasaki, T. Anion-Exchangeable Layered Materials Based on Rare-Earth Phosphors: Unique Combination of Rare-Earth Host and Exchangeable Anions. *Acc. Chem. Res.* **2010**, *43*, 1177−1185.
(51) Colinas, I. R.; Inglis, K. K.; Blanc, F.; Oliver, S. R. J. Anion Exchange Dynamics in the Capture of Perchlorate by a Cationic Ag-based MOF. *Dalton Trans.* **2017**, *46*, 5320−5325.
(52) Shi, P.-F.; Zhao, B.; Xiong, G.; Hou, Y.-L.; Cheng, P. Fast Capture and Separation of, and Luminescent Probe for, Pollutant Chromate using a Multi-Functional Cationic Heterometal-Organic Framework. *Chem. Commun.* **2012**, *48*, 8231−8233.
(53) Rapti, S.; Pournara, A.; Sarma, D.; Papadas, I. T.; Armatas, G. S.; Tsipis, A. C.; Lazarides, T.; Kanatzidis, M. G.; Manos, M. J. Selective Capture of Hexavalent Chromium from an Anion-Exchange Column of Metal-Organic Resin-Alginic Acid Composite. *Chem. Sci.* **2016**, *7*, 2427−2436.
(54) Oliver, S. R. J. Cationic Inorganic Materials for Anionic Pollutant Trapping and Catalysis. *Chem. Soc. Rev.* **2009**, *38*, 1868−1881.
(55) Wang, S.; Alekseev, E. V.; Diwu, J.; Casey, W. H.; Phillips, B. L.; Depmeier, W.; Albretch-Schmitt, T. E. NDTB-1: A Super-tetrahedral Cationic Framework that Removes TcO_4^- from Solution. *Angew. Chem., Int. Ed.* **2010**, *49*, 1057−1060.
(56) Fu, H.-R.; Xu, Z.-X.; Zhang, J. Water-Stable Metal-Organic Frameworks for Fast and High Dichromate Trapping via Single-Crystal-to-Single-Crystal Ion Exchange. *Chem. Mater.* **2015**, *27*, 205−210.

DOI: 10.1021/acsami.8b15946
ACS Appl. Mater. Interfaces 2019, 11, 3181−3188

(57) Liu, W.; Wang, Y.; Bai, Z.; Li, Y.; Wang, Y.; Chen, L.; Xu, L.; Diwu, J.; Chai, Z.; Wang, S. Hydrolytically Stable Luminescent Cationic Metal Organic Framework for Highly Sensitive and Selective Sensing of Chromate Anions in Natural Water Systems. *ACS Appl. Mater. Interfaces* **2017**, *9*, 16448−16457.
(58) Drinking Water Requirements for States and Public Water Systems. United States Environmental Protection Agency. https://www.epa.gov/dwreginfo.
(59) Robinson, F.; Zaworotko, M. J. Triple Interpenetration in [Ag(4,4′-bipyridine)][NO_3], a Cationic Polymer with a Three-Dimensional Motif Generated by Self-Assembly of 'T-Shaped' Building Blocks. *J. Chem. Soc., Chem. Commun.* **1995**, 2413−2414.
(60) Fei, H.; Rogow, D. L.; Oliver, S. R. J. Reversible Anion Exchange and Catalytic Properties of Two Cationic Metal-Organic Frameworks Based on Cu(I) and Ag(I). *J. Am. Chem. Soc.* **2010**, *132*, 7202−7209.
(61) Eddaoudi, M.; Moler, D. B.; Li, H.; Chen, B.; Reineke, T. M.; O'Keeffe, M.; Yaghi, O. M. Modular Chemistry: Secondary Building Units as a Basis for the Design of Highly Porous and Robust Metal-Organic Carboxylate Frameworks. *Acc. Chem. Res.* **2001**, *34*, 319−330.
(62) Zhao, X.; Mao, C.; Luong, K. T.; Lin, Q.; Zhai, Q.-G.; Feng, P.; Bu, X. Framework Cationization by Preemptive Coordination of Open Metal Sites for Anion Exchange Encapsulation of Nucleotides and Coenzymes. *Angew. Chem., Int. Ed.* **2016**, *55*, 2768−2772.
(63) Mao, C.; Kudla, R. A.; Zuo, F.; Zhao, X.; Mueller, L. J.; Bu, X.; Feng, P. Anion Stripping as a General Method to Create Cationic Porous Framework with Mobile Anions. *J. Am. Chem. Soc.* **2014**, *136*, 7579−7582.
(64) Aharen, T.; Habib, F.; Korobkov, I.; Burchell, T. J.; Guillet-Nicolas, R.; Kleiz, F.; Murugesu, M. Novel Co-based Metal-Organic Frameworks and their Magnetic Properties using Asymmetrically Binding 4-(4′-carboxyphenyl)-1,2,4-triazole. *Dalton Trans.* **2013**, *42*, 7795−7802.
(65) Zhai, Q.-G.; Bu, X.; Mao, C.; Zhao, X.; Daemen, L.; Cheng, Y.; Ramirez-Cuesta, A. J.; Feng, P. An Ultra-Tunable Platform for Molecular Engineering of High-Performance Crystalline Porous Materials. *Nat. Commun.* **2016**, *7*, No. 13645.
(66) Zheng, S.-T.; Zhao, X.; Lau, S.; Fuhr, A.; Feng, P.; Bu, X. Entrapment of Metal Clusters in Metal-Organic Frameworks Channels by Extended Hooks Anchored at Open Metal Sites. *J. Am. Chem. Soc.* **2013**, *135*, 10270−10273.
(67) Custelcean, R.; Moyer, B. A. Anion Separation with Metal-Organic Frameworks. *Eur. J. Inorg. Chem.* **2007**, *2007*, 1321−1340.
(68) Carlucci, L.; Ciani, G.; Maggini, S.; Proserpio, D. M.; Visconti, M. Heterometallic Modular Metal-Organic 3D Frameworks Assembled via New Tris-β-Diketonate Metalloligands: Nanoporous Materials for Anion Exchange and Scaffolding of Selected Anionic Guests. *Chem. - Eur. J.* **2010**, *16*, 12328−12341.
(69) Zhao, X.; Bu, X.; Wu, T.; Zheng, S.-T.; Wang, L.; Feng, P. Selective Anion Exchange with Nanogated Isoreticular Positive Metal-Organic Frameworks. *Nat. Commun.* **2013**, *4*, No. 2344.
(70) Hasan, Z.; Jhung, S. H. Removal of Hazardous Organics from Water using Metal-Organic Frameworks (MOFs): Plausible Mechanisms for Selective Adsorptions. *J. Hazard. Mater.* **2015**, *283*, 329−339.
(71) Khan, N. A.; Hasan, Z.; Jhung, S. H. Adsorptive Removal of Hazardous Materials using Metal-Organic Frameworks (MOFs): A Review. *J. Hazard. Mater.* **2013**, *244*−*245*, 444−456.
(72) Sudik, A. C.; Côté, A. P.; Yaghi, O. M. Metal-Organic Frameworks Based on Trigonal Prismatic Building Blocks and the New "acs" Topology. *Inorg. Chem.* **2005**, *44*, 2998−3000.
(73) Wongsakulphasatch, S.; Nouar, F.; Rodriguez, J.; Scott, L.; Le Guillouzer, C.; Devic, T.; Horcajada, P.; Grenèche, J.-M.; Llewellyn, P. L.; Vimont, A.; Clet, G.; Daturi, M.; Serre, C. Direct Accessibility of Mixed-Metal (III/II) Acid Sites Through the Rational Synthesis of Porous Metal Carboxylates. *Chem. Commun.* **2015**, *51*, 10194−10197.
(74) Gao, Q.; Zhao, X.-L.; Chang, Z.; Xu, J.; Bu, X.-H. Structural Stabilization of a Metal-Organic Framework for Gas Sorption Investigation. *Dalton Trans.* **2016**, *45*, 6830−6833.
(75) Lin, J.-B.; Shimizu, G. K. H. Pyridinium Linkers and Mixed Anions in Cationic Metal-Organic Frameworks. *Inorg. Chem. Front.* **2014**, *1*, 302−305.

DOI: 10.1021/acsami.8b15946
ACS Appl. Mater. Interfaces 2019, 11, 3181−3188